Appl. Math. Mech. -Engl. Ed., **39**(3), 335–352 (2018)

Applied Mathematics and Mechanics (English Edition)

https://doi.org/10.1007/s10483-018-2309-9

Static deformation of a multilayered one-dimensional hexagonal quasicrystal plate with piezoelectric effect*

Tuoya SUN, Junhong GUO†, Xiaoyan ZHANG

Department of Mechanics, Inner Mongolia University of Technology, Hohhot 010051, China

(Received May 22, 2017 / Revised Sept. 12, 2017)

Abstract Quasicrystals (QCs) are sensitive to the piezoelectric (PE) effect. This paper studies static deformation of a multilayered one-dimensional (1D) hexagonal QC plate with the PE effect. The exact closed-form solutions of the extended displacement and traction for a homogeneous piezoelectric quasicrystal (PQC) plate are derived from an eigensystem. The general solutions for multilayered PQC plates are then obtained using the propagator matrix method when mechanical and electrical loads are applied on the top surface of the plate. Numerical examples for several sandwich plates made up of PQC, PE, and QC materials are provided to show the effect of stacking sequence on phonon, phason, and electric fields under mechanical and electrical loads, which is useful in designing new composites for engineering structures.

Key words quasicrystal (QC), piezoelectric (PE) effect, multilayered plate, exact solution, static deformation

Chinese Library Classification O343.8
2010 Mathematics Subject Classification 52C23, 74K20, 74B05

1 Introduction

Quasicrystals (QCs) in the Al-Mn phase were discovered firstly in 1982 by Shechtman et al.[1], which exhibit the forbidden rotational symmetry in the conventional crystallography and lack translational symmetry. The ordered but aperiodic atomic arrangement in QCs enables them to display some attractive properties[2–5], such as high hardness, high wear resistance, low thermal conductivity, low electrical conductivity, low surface energy, and high infra-red absorption. Due to these special properties, QCs have many potential applications[6–9], including thermal barrier coatings, wear resistant coatings, and reinforcements in composites and thin film. The multilayered plate model offers guidance in understanding the deformation of QC coatings or thin film.

A one-dimensional (1D) QC refers to a three-dimensional (3D) structure with atomic arrangement quasi-periodically in one direction and periodically in the plane perpendicular to

∗ Citation: Sun, T. Y., Guo, J. H., and Zhang, X. Y. Static deformation of a multilayered one-dimensional hexagonal quasicrystal plate with piezoelectric effect. *Applied Mathematics and Mechanics* (*English Edition*), **39**(3), 335–352 (2018) https://doi.org/10.1007/s10483-018-2309-9

† Corresponding author, E-mail: jhguo@imut.edu.cn

Project supported by the National Natural Science Foundation of China (Nos. 11502123 and 11262012) and the Natural Science Foundation of Inner Mongolia Autonomous Region of China (No. 2015JQ01)

that direction. For the plate model in QCs, Gao et al.[10] applied the reciprocal theorem to consider the plate bending of 1D hexagonal QCs. Furthermore, Gao and Ricoeur[11] established a refined theory of thick plates for 1D QCs. Sladek et al.[12] used the meshless Pethov-Galerkin method to analyze the bending problem in 1D orthorhombic QCs under static and transient dynamic loads. Waksmanski et al.[13] obtained an exact closed-form solution of free vibration of a simply-supported and multilayered 1D QC plate by using the pseudo-Stroh formulation and propagator matrix method. Yang et al.[14–15] derived an exact closed-form solution for a simply-supported and multilayered two-dimensional (2D) decagonal QC plate and 1D orthorhombic QC plate by utilizing the pseudo-Stroh formalism.

The studies showed that piezoelectricity is an important physical property of QCs[16–20]. The inherent piezoelectric (PE) coupling effect of QCs has attracted much attention, and exciting advances have been achieved. For example, Altay and Dökmeci[21] addressed the 3D basic equations of piezoelectric quasicrystals (PQCs). Li et al.[22] obtained the 3D general solutions to a static problem of 1D hexagonal PQCs by utilizing the operator theory. Yu et al.[23] derived the governing equations of the plane electroelastic problem of 1D PQCs and their general solutions. Based on these theories, the eletroelastic behaviors of 1D PQC involving dislocations[24–25], cracks[23–26], holes[27–28], and inclusions[29–30] have been investigated extensively. More recently, by using an extended dislocation layer method, Tupholme[31] derived the closed-form expressions of the stress and electric fields for a moving non-constantly loaded antiplane, Griffith-type strip crack in 1D PQCs. Yang et al.[32] used the pseudo-Stroh formalism and propagator matrix method to present an exact elastic analysis of a multilayered 2D decagonal QC plate subject to patch loading with simply-supported boundary conditions.

As mentioned above, although some plate models in QCs were conducted, to the best of the authors' knowledge, the static deformation of 1D PQC plate in a 3D finite space has not been reported in the literature. In fact, PQC plates process the coupling effect among phonon, phason, and electric fields, which is superior to QC plates with phonon-phason coupling in engineering practice. To better understand the unique physical properties of QCs to meet our increasing demands or new materials, it is of significance to study multilayered PQC plates. Therefore, in this work, we derive an exact closed-form solution of static deformation for 3D multilayered plates made of 1D PQCs, QCs, and PE with simply-supported boundary conditions.

2 Problem description and basic equations

We consider a simply-supported, transversely isotropic, and multilayered 1D hexagonal PQC plate with horizontal dimensions L_x and L_y and a total thickness H, as shown in Fig. 1. A Cartesian coordinate system is placed on the horizontal Ox_1x_2-plane of the bottom surface, and the positive x_3-direction is along the thickness of the plate. The horizontal Ox_1x_2-plane is the

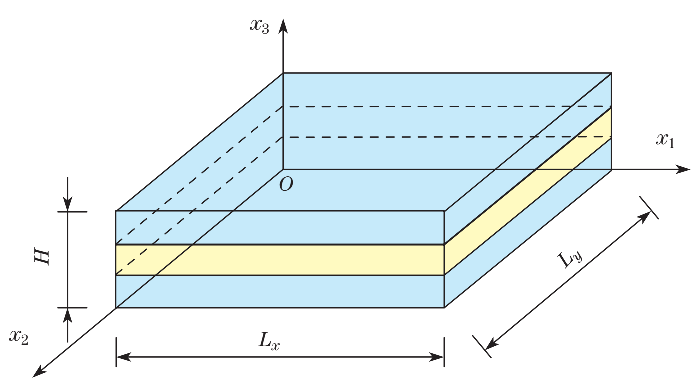

Fig. 1 A multilayered 1D hexagonal PQC plate

periodic plane, and both the quasi-periodic direction and the electric poling direction are along the x_3-axis. There are N layers with the thickness $h_j = z_j - z_{j-1}$ ($j = 1, 2, \cdots, N$), and each layer is bonded perfectly on its interfaces. Thus, we assume that the extended displacement and traction are continuous across the interfaces, i.e.,

$$\begin{cases} (u_i)_j = (u_i)_{j+1}, \quad (w_3)_j = (w_3)_{j+1}, \quad (\phi)_j = (\phi)_{j+1}, \\ (\sigma_{i3})_j = (\sigma_{i3})_{j+1}, \quad (H_{33})_j = (H_{33})_{j+1}, \quad (D_3)_j = (D_3)_{j+1}. \end{cases} \tag{1}$$

Furthermore, the simply-supported boundary conditions can be written as

$$\begin{cases} x_1 = 0, \quad x_1 = L_x: \quad u_2 = u_3 = w_3 = \phi = 0, \\ x_2 = 0, \quad x_2 = L_y: \quad u_1 = u_3 = w_3 = \phi = 0, \end{cases} \tag{2}$$

where $x_1 = 0$ and $x_1 = L_x$ denote the left and right edges of the plate, respectively, and $x_2 = 0$ and $x_2 = L_y$ denote the back and front edges of the plate, respectively. At these edges, the displacements u_i ($i = 1, 2, 3$) of the phonon field, the displacement w_3 of the phason field, and the electric potential ϕ are zeros.

The basic equations for static deformation of PQCs presented by Altay and Dökmeci[21] include the equilibrium equations

$$\sigma_{ij,j} = 0, \quad H_{ij,j} = 0, \quad D_{i,i} = 0, \tag{3}$$

the gradient equations

$$\varepsilon_{ij} = \frac{1}{2}(u_{i,j} + u_{j,i}), \quad \omega_{ij} = w_{i,j}, \quad E_i = -\phi_{,i}, \tag{4}$$

and the constitutive equations

$$\begin{cases} \sigma_{ij} = C_{ijkl}\varepsilon_{kl} + R_{ijkl}\omega_{kl} - e_{kij}E_k, \\ H_{ij} = R_{klij}\varepsilon_{kl} + K_{ijkl}\omega_{kl} - d_{kij}E_k, \\ D_i = e_{ijk}\varepsilon_{jk} + d_{ijk}\omega_{jk} + \lambda_{ij}E_j. \end{cases} \tag{5}$$

In (1)–(5), a comma denotes differentiation with respect to x_i ($i = 1, 2, 3$), repeated indices imply summation (from 1 to 3), σ_{ij}, ε_{ij}, and u_i are the components of the stress, strain, and displacement of the phonon field, respectively, H_{ij}, ω_{ij}, and w_i are the components of the stress, strain, and displacement of the phason field, respectively, D_i, E_i, and ϕ are the electric displacements, electric fields, and electric potential, respectively, C_{ijkl} and K_{ijkl} are the elastic constants of the phonon field and phason field, respectively, R_{ijkl} are the phonon-phason coupling elastic constants, e_{ijk} and d_{ijk} are the PE coefficients, and λ_{ij} is the dielectric permittivity.

3 General solutions for a homogeneous 1D hexagonal PQC plate

To satisfy the simply-supported boundary conditions (2), the general solutions of the extended displacement vector for a homogeneous PQC plate can be assumed in the form of

$$\boldsymbol{u} \equiv \begin{bmatrix} u_1 \\ u_2 \\ u_3 \\ w_3 \\ \phi \end{bmatrix} = \mathrm{e}^{sz} \begin{bmatrix} a_1 \cos(px)\sin(qy) \\ a_2 \sin(px)\cos(qy) \\ a_3 \sin(px)\sin(qy) \\ a_4 \sin(px)\sin(qy) \\ a_5 \sin(px)\sin(qy) \end{bmatrix}, \tag{6}$$

where

$$p=n\pi/L_x,\quad q=m\pi/L_y, \tag{7}$$

in which n and m are two positive integers. Also in (6), s is the eigenvalue, and $a_1,a_2,\cdots,a_5$ are unknown constants to be determined. Notice that by taking the summation over n and m values, we then have the general solution in terms of 2D Fourier series expansion.

From the gradient equation (4), the constitutive equation (5), and the general solution (6) of the extended displacement, the extended traction vector can be expressed as

$$\boldsymbol{t}\equiv\begin{bmatrix}\sigma_{13}\\ \sigma_{23}\\ \sigma_{33}\\ H_{33}\\ D_3\end{bmatrix}=\mathrm{e}^{sz}\begin{bmatrix}b_1\cos(px)\sin(qy)\\ b_2\sin(px)\cos(qy)\\ b_3\sin(px)\sin(qy)\\ b_4\sin(px)\sin(qy)\\ b_5\sin(px)\sin(qy)\end{bmatrix}. \tag{8}$$

Two group coefficients of (6) and (8) are written in the forms of vectors $\boldsymbol{a}=[a_1,a_2,\cdots,a_5]^{\mathrm{T}}$ and $\boldsymbol{b}=[b_1,b_2,\cdots,b_5]^{\mathrm{T}}$ with the following relationship:

$$\boldsymbol{b}=(-\boldsymbol{R}^{\mathrm{T}}+s\boldsymbol{T})\boldsymbol{a}=-\frac{1}{s}(\boldsymbol{Q}+s\boldsymbol{R})\boldsymbol{a}, \tag{9}$$

where the superscript T denotes matrix transpose, and the matrices $\boldsymbol{R}$, $\boldsymbol{T}$, and $\boldsymbol{Q}$ are

$$\boldsymbol{R}=\begin{bmatrix}0&0&c_{13}p&R_{31}p&e_{31}p\\ 0&0&c_{13}q&R_{31}q&e_{31}q\\ -c_{44}p&-c_{44}q&0&0&0\\ -R_{24}p&-R_{24}q&0&0&0\\ -e_{15}p&-e_{15}q&0&0&0\end{bmatrix}, \tag{10}$$

$$\boldsymbol{T}=\begin{bmatrix}c_{44}&0&0&0&0\\ 0&c_{44}&0&0&0\\ 0&0&c_{33}&R_{33}&e_{33}\\ 0&0&R_{33}&K_{33}&d_{33}\\ 0&0&e_{33}&d_{33}&-\lambda_{33}\end{bmatrix}, \tag{11}$$

$$\boldsymbol{Q}=[\boldsymbol{Q}_1,\boldsymbol{Q}_2], \tag{12}$$

in which

$$\boldsymbol{Q}_1=\begin{bmatrix}-c_{11}p^2-c_{66}q^2&-c_{12}pq-c_{66}pq\\ -c_{66}pq-c_{12}pq&-c_{66}p^2-c_{11}q^2\\ 0&0\\ 0&0\\ 0&0\end{bmatrix},$$

$$\boldsymbol{Q}_2=\begin{bmatrix}0&0&0\\ 0&0&0\\ -c_{44}(p^2+q^2)&-R_{24}(p^2+q^2)&-e_{15}(p^2+q^2)\\ -R_{24}(p^2+q^2)&-K_{11}(p^2+q^2)&-d_{11}(p^2+q^2)\\ -e_{15}(p^2+q^2)&-d_{11}(p^2+q^2)&\lambda_{11}(p^2+q^2)\end{bmatrix},$$

where the short notations for the subscripts are used from 4 to 2, i.e., 11→1, 22→2, 33→3, 23→4, 31→5, and 12→6. The latter two numbers of e_{kij} and d_{kij} are also simplified similarly.

Substituting the extended traction vector in (8) into the equilibrium equation (3), we have

$$\boldsymbol{Q}\boldsymbol{a} + s\boldsymbol{b} + s\boldsymbol{R}\boldsymbol{a} = \boldsymbol{0}. \tag{13}$$

From (9) and (13), the final governing equation can be derived as

$$(\boldsymbol{Q} + s(\boldsymbol{R} - \boldsymbol{R}^{\mathrm{T}}) + s^2\boldsymbol{T})\boldsymbol{a} = \boldsymbol{0}. \tag{14}$$

Similar to the method of Pan[33], (9) and (14) can be transformed to a linear eigensystem as follows:

$$\boldsymbol{N}\begin{bmatrix} \boldsymbol{a} \\ \boldsymbol{b} \end{bmatrix} = s\begin{bmatrix} \boldsymbol{a} \\ \boldsymbol{b} \end{bmatrix}, \tag{15}$$

where

$$\boldsymbol{N} = \begin{bmatrix} \boldsymbol{T}^{-1}\boldsymbol{R}^{\mathrm{T}} & \boldsymbol{T}^{-1} \\ -\boldsymbol{Q} - \boldsymbol{R}\boldsymbol{T}^{-1}\boldsymbol{R}^{\mathrm{T}} & -\boldsymbol{R}\boldsymbol{T}^{-1} \end{bmatrix}. \tag{16}$$

If we solve the eigenvalues and eigenvectors from (15), the general solution for a 1D homogenous PQC plate can be obtained as

$$\begin{bmatrix} \boldsymbol{u} \\ \boldsymbol{t} \end{bmatrix} = \begin{bmatrix} \boldsymbol{A} \\ \boldsymbol{B} \end{bmatrix} \langle \mathrm{e}^{s^* z} \rangle \boldsymbol{K}. \tag{17}$$

In (17), $\boldsymbol{K}$ is a constant vector to be determined by the external loads on the surfaces of the plates, and the matrices $\boldsymbol{A}$ and $\boldsymbol{B}$ and the diagonal matrix are

$$\begin{cases} \boldsymbol{A} = [\boldsymbol{a}_1,\ \boldsymbol{a}_2,\ \cdots,\ \boldsymbol{a}_{10}], \quad \boldsymbol{B} = [\boldsymbol{b}_1,\ \boldsymbol{b}_2,\ \cdots,\ \boldsymbol{b}_{10}], \\ \langle \mathrm{e}^{s^* z} \rangle = \mathrm{diag}[\mathrm{e}^{s_1 z},\ \mathrm{e}^{s_2 z}, \cdots, \mathrm{e}^{s_{10} z}]. \end{cases} \tag{18}$$

4 Exact closed-form solution of multilayered PQC plates

According to the boundary condition of the bottom surface of plate, we can obtain the constant vector $\boldsymbol{K}$ from (17), i.e.,

$$\boldsymbol{K} = \begin{bmatrix} \boldsymbol{A} \\ \boldsymbol{B} \end{bmatrix}^{-1} \begin{bmatrix} \boldsymbol{u} \\ \boldsymbol{t} \end{bmatrix}_0. \tag{19}$$

Substituting (19) into (17), the general solutions of the extended displacement and traction become

$$\begin{bmatrix} \boldsymbol{u} \\ \boldsymbol{t} \end{bmatrix}_z = \boldsymbol{P}(z) \begin{bmatrix} \boldsymbol{u} \\ \boldsymbol{t} \end{bmatrix}_0, \tag{20}$$

where $\boldsymbol{P}(z)$ is the propagator matrix, i.e.,

$$\boldsymbol{P}(z) = \begin{bmatrix} \boldsymbol{A} \\ \boldsymbol{B} \end{bmatrix} \langle \mathrm{e}^{s^* z} \rangle \begin{bmatrix} \boldsymbol{A} \\ \boldsymbol{B} \end{bmatrix}^{-1}. \tag{21}$$

Making use of the following characteristic of the propagator matrix[33]:

$$\boldsymbol{P}(z_3 - z_1) = \boldsymbol{P}(z_3 - z_2)\boldsymbol{P}(z_2 - z_1), \tag{22}$$

we can propagate the solution from the bottom surface $z = 0$ to the top surface $z = H$ of the multilayered PQC plate by using the propagating relation (20) repeatedly, i.e.,

$$\begin{bmatrix} \boldsymbol{u} \\ \boldsymbol{t} \end{bmatrix}_H = \boldsymbol{Q} \begin{bmatrix} \boldsymbol{u} \\ \boldsymbol{t} \end{bmatrix}_0, \tag{23}$$

where

$$\boldsymbol{Q} = \boldsymbol{P}_N(h_N)\boldsymbol{P}_{N-1}(h_{N-1}) \cdots \boldsymbol{P}_2(h_2)\boldsymbol{P}_1(h_1). \tag{24}$$

To solve the boundary value problem above, the extended stress boundary conditions should be considered. If the top surface of the plate is only subject to the electrical-mechanical loads and the bottom surface is free of traction, we have

$$\begin{cases} \boldsymbol{t}(H) = [0, 0, \sigma_0 \sin(px) \sin(qy), 0, D_0 \sin(px) \sin(qy)]^{\mathrm{T}}, \\ \boldsymbol{t}(0) = [0, 0, 0, 0, 0]^{\mathrm{T}}. \end{cases} \tag{25}$$

From (23) and (25), $\boldsymbol{u}(0)$ can be obtained as

$$\boldsymbol{u}(0) = [\boldsymbol{Q}_{21}]^{-1}\boldsymbol{t}(H), \tag{26}$$

where $\boldsymbol{Q}_{21}$ is the submatrix of the propagator matrix $\boldsymbol{Q}$ in (24).

Thus, the general solutions of the extended displacement and traction are solved completely from (20), (25), and (26).

5 Numerical examples

In the numerical analysis, we consider several sandwich plates made up of PQC1, PQC2, QC (Al-Ni-Co), and PE ($BaTiO_3$) materials, where the material properties of these materials are given in Tables 1 and 2. The effect of stacking sequence for different materials on the phonon, phason, and electric fields is analyzed, which is very useful in designing new laminate composites for engineering structures. Yang et al.[32] comprehensively presented an exact electroelastic solution of a multilayered 2D decagonal QC plate subject to three different cases of surface patch loading, such as transverse shear force, normal force, and electric potential. In their analysis, the dimensions of the sandwich plates were taken as $L_x = L_y = 3 \times 10^{-2}$ m and $H = 3 \times 10^{-3}$ m, and the responses for fixed horizontal coordinates $(x, y) = (0.5L_x, 0.5L_y)$ were considered. In our numerical analysis, the dimensions of the plate are $L_x = L_y = 1$ m and $H = 0.3$ m. The three layers have equal thickness of 0.1 m. We take $\sigma_0 = 1$ N/m^2 and $D_0 = 1$ C/m^2 with $n = m = 1$, and consider the responses for fixed horizontal coordinates $(x, y) = (0.75L_x,\ 0.25L_y)$.

Table 1 Material coefficients of PQC1 and PQC2[22,30]

Material coefficient		PQC1	PQC2	Material coefficient		PQC1	PQC2
C_{ij}	C_{11}/(N·m^{-2})	150×10^9	150×10^9	R_{ij}	R_{31}/(N·m^{-2})	-1.50×10^9	-1.50×10^9
	C_{12}/(N·m^{-2})	100×10^9	100×10^9		R_{33}/(N·m^{-2})	1.20×10^9	1.20×10^9
	C_{13}/(N·m^{-2})	90×10^9	90×10^9		R_{24}/(N·m^{-2})	-1.10×10^9	1.20×10^9
	C_{33}/(N·m^{-2})	130×10^9	130×10^9	e_{ij}	e_{31}/(C·m^{-2})	-0.160	-0.160
	C_{44}/(N·m^{-2})	35×10^9	50×10^9		e_{33}/(C·m^{-2})	0.347	0.347
	$C_{66} = (C_{11} - C_{12})/2$				e_{15}/(C·m^{-2})	17.000	-0.138
K_{ij}	K_{11}/(N·m^{-2})	0.24×10^9	0.30×10^9	d_{ij}	d_{11}/(C·m^{-2})	-0.100	-0.160
	K_{33}/(N·m^{-2})	0.18×10^9	0.18×10^9		d_{33}/(C·m^{-2})	0.350	0.350
λ_{ij}	λ_{11}/(C^2·N^{-1}·m^{-2})	1.51×10^{-12}	82.6×10^{-12}				
	λ_{33}/(C^2·N^{-1}·m^{-2})	90.30×10^{-12}	90.3×10^{-12}				

Table 2 Material coefficients of Al-Ni-Co[34] and $BaTiO_3$[35]

Material coefficient		QC	PE	Material coefficient		QC	PE
C_{ij}	$C_{11}/(\mathrm{N{\cdot}m^{-2}})$	234.33×10^9	166×10^9	R_{ij}	$R_{31}/(\mathrm{N{\cdot}m^{-2}})$	8.846×10^9	–
	$C_{12}/(\mathrm{N{\cdot}m^{-2}})$	57.41×10^9	77×10^9		$R_{33}/(\mathrm{N{\cdot}m^{-2}})$	8.846×10^9	–
	$C_{13}/(\mathrm{N{\cdot}m^{-2}})$	66.63×10^9	78×10^9		$R_{24}/(\mathrm{N{\cdot}m^{-2}})$	8.846×10^9	–
	$C_{33}/(\mathrm{N{\cdot}m^{-2}})$	232.22×10^9	162×10^9	e_{ij}	$e_{31}/(\mathrm{C{\cdot}m^{-2}})$	–	-4.4
	$C_{44}/(\mathrm{N{\cdot}m^{-2}})$	70.19×10^9	43×10^9		$e_{33}/(\mathrm{C{\cdot}m^{-2}})$	–	18.6
	$C_{66}=(C_{11}-C_{12})/2$				$e_{15}/(\mathrm{C{\cdot}m^{-2}})$	–	11.6
K_{ij}	$K_{11}/(\mathrm{N{\cdot}m^{-2}})$	0.24×10^9	0.30×10^9		$e_{24}/(\mathrm{C{\cdot}m^{-2}})$	–	11.6
	$K_{33}/(\mathrm{N{\cdot}m^{-2}})$	24×10^9	–	d_{ij}	$d_{11}/(\mathrm{C{\cdot}m^{-2}})$	–	–
λ_{ij}	$\lambda_{11}/(\mathrm{C^2{\cdot}N^{-1}{\cdot}m^{-2}})$	–	11.2×10^{-9}		$d_{33}/(\mathrm{C{\cdot}m^{-2}})$	–	–
	$\lambda_{33}/(\mathrm{C^2{\cdot}N^{-1}{\cdot}m^{-2}})$	–	12.6×10^{-9}				

It should be noted that in QC materials, only phonon and phason fields exist and there is no electric field. Thus, in PQC1/QC/PQC1, QC/PQC1/QC, PE/QC/PE, and QC/PE/QC plates, the dielectric constants λ_{ij} should be zero in the QC layer. To avoid the singularity of matrices in calculation, we use a small λ_{ij} value (10^{-11} of the corresponding λ_{ij}) in the QC layer. Similarly, the elastic constants K_{ij} of phason field in PE materials are taken in this way.

Example 1 The plate subject to mechanical loads on the top surface

Figures 2 and 3 show the variation of displacement of phonon field for four different sandwich plates along the thickness direction of the plates under mechanical loads. It is clear that the stacking sequence of the plates greatly affects the displacement. If the upper and lower layers

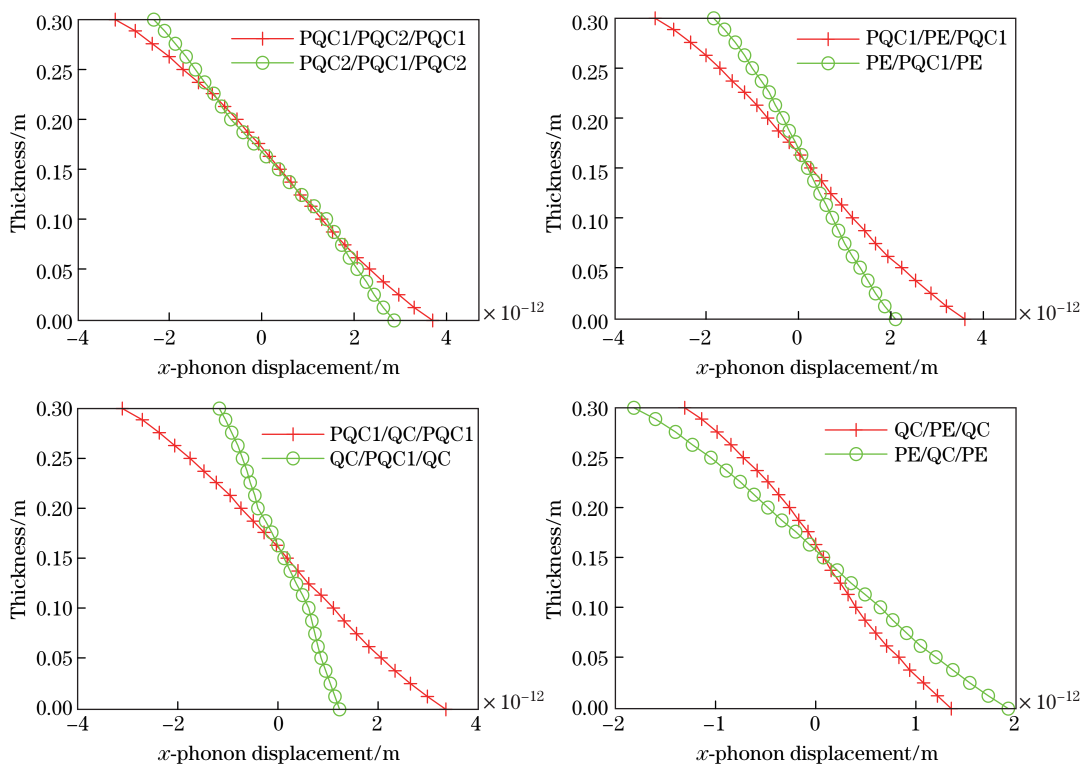

Fig. 2 Variation of phonon displacement $u_x(=u_y)$ along the thickness direction of the plate

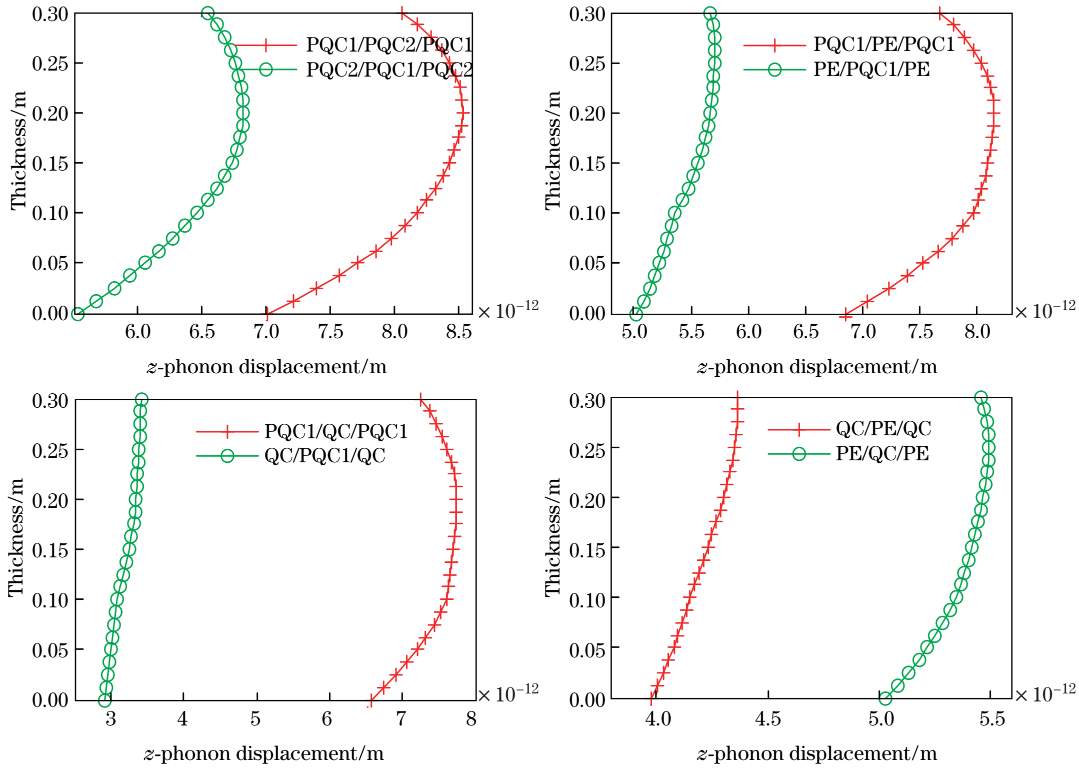

Fig. 3 Variation of phonon displacement u_z along the thickness direction of the plate

are QCs, the deformation of all sandwich plates can be reduced. Thus, QCs are commonly used as the thermal barrier coatings, wear resistant coatings, and reinforcements in composites to enhance the mechanical property of the other composite materials[6–9]. However, PE can only improve the mechanical property of PQC plates.

Figure 4 shows the variation of displacement of the phason field for four different sandwich plates along the thickness direction of the plate under mechanical loads. We find from Fig. 4 that the displacement of the phason field in the PQC2 and QC layers is almost constant. The displacement of phason field is kinked across the interfaces, which is different from the displacement of phonon field. It should be pointed out that the phason displacement in the non-QC layer is set to be zero[13–15] since there is no physical meaning for it in the non-QC layer. Thus, we also set the phason displacement in the PE layer to be zero. However, for the phason stress in the PE layer, it is always zero in the PE layer as expected.

Figure 5 shows the electric potential ϕ for four different sandwich plates along the thickness direction of the plate under mechanical loads. It is observed that the electric potential for the sandwich plates QC/PE/QC and PE/QC/PE reaches its maximum at the interfaces, while the electric potential of the other sandwich plates reaches its maximum on the surfaces of plates.

Figure 6 shows the variation of the shear stress σ_{xz} of phonon field for four different sandwich plates along the thickness direction of the plate under mechanical loads. The stacking sequence nearly has no effect on the shear stress except for the middle layer. For the normal stress σ_{zz} of phonon field (see Fig. 7), there is little difference for four different sandwich plates, which is also independent of the stacking sequence.

Figure 8 shows the variation of the normal stress H_{zz} of phason field for four different sandwich plates along the thickness direction of the plate under mechanical loads. The stress of the phason field shows a very different variation as compared with the stress of the phonon field (see Fig. 7). Meanwhile, the stacking sequence greatly affects the stress of the phason field. The following features can be further found from Fig. 8. (i) The stress of the phason field is

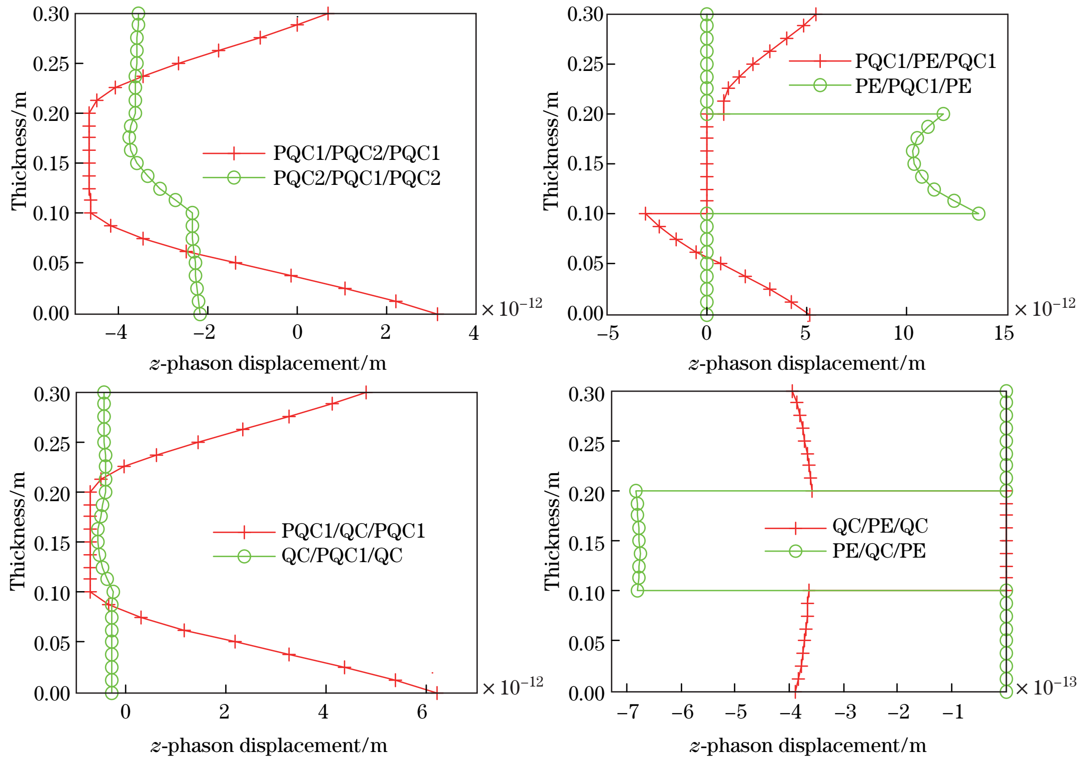

Fig. 4 Variation of phason displacement w_z along the thickness direction of the plate

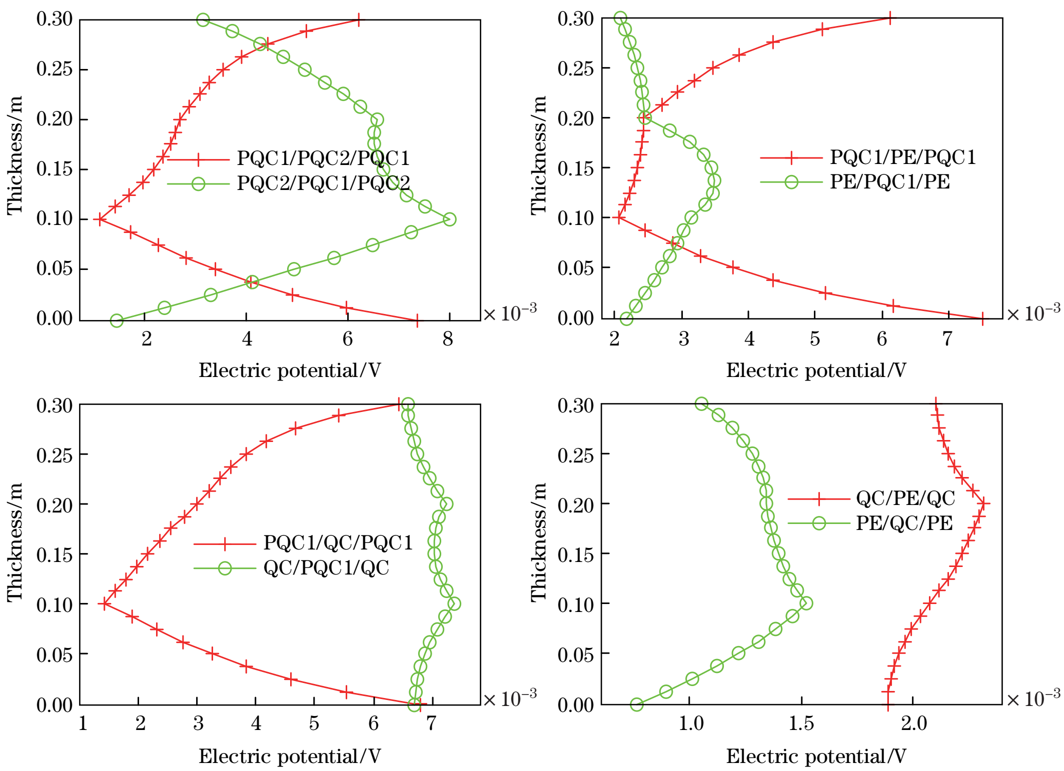

Fig. 5 Variation of electric potential ϕ along the thickness direction of the plate

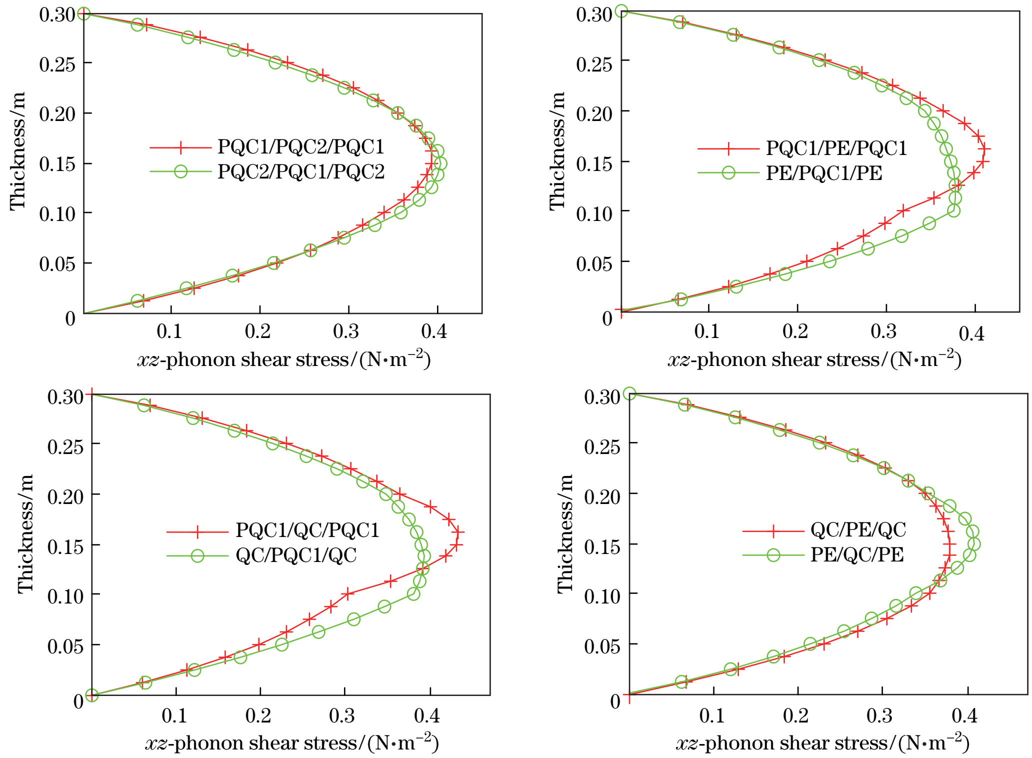

Fig. 6 Variation of phonon shear stress σ_{xz} along the thickness direction of the plate

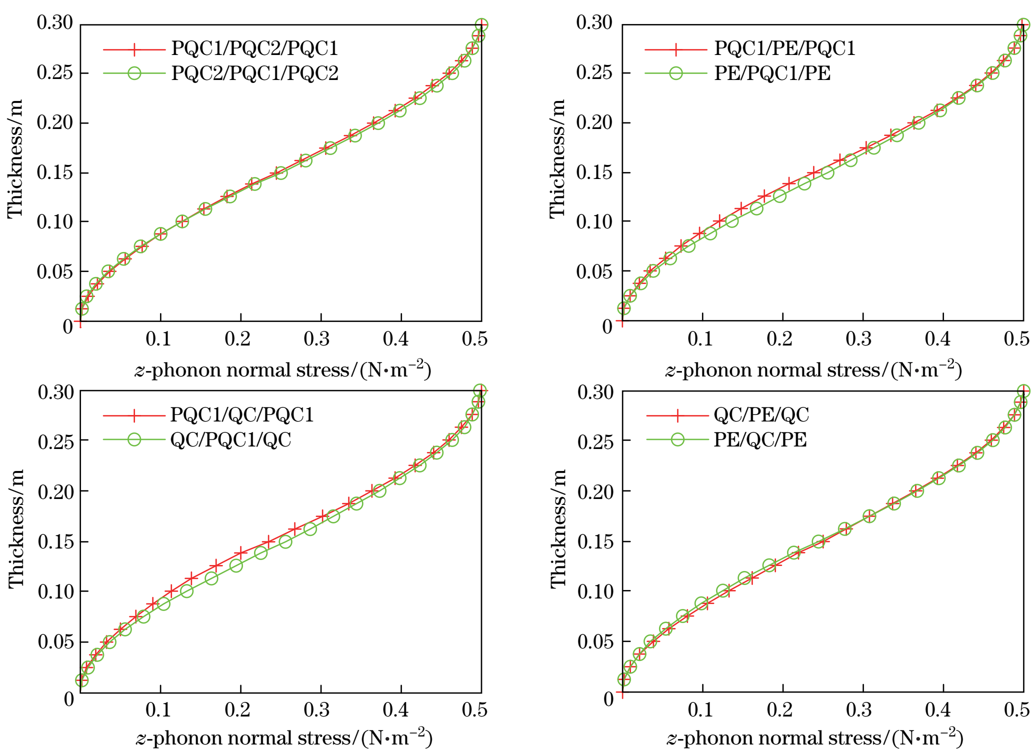

Fig. 7 Variation of phonon normal stress σ_{zz} along the thickness direction of the plate

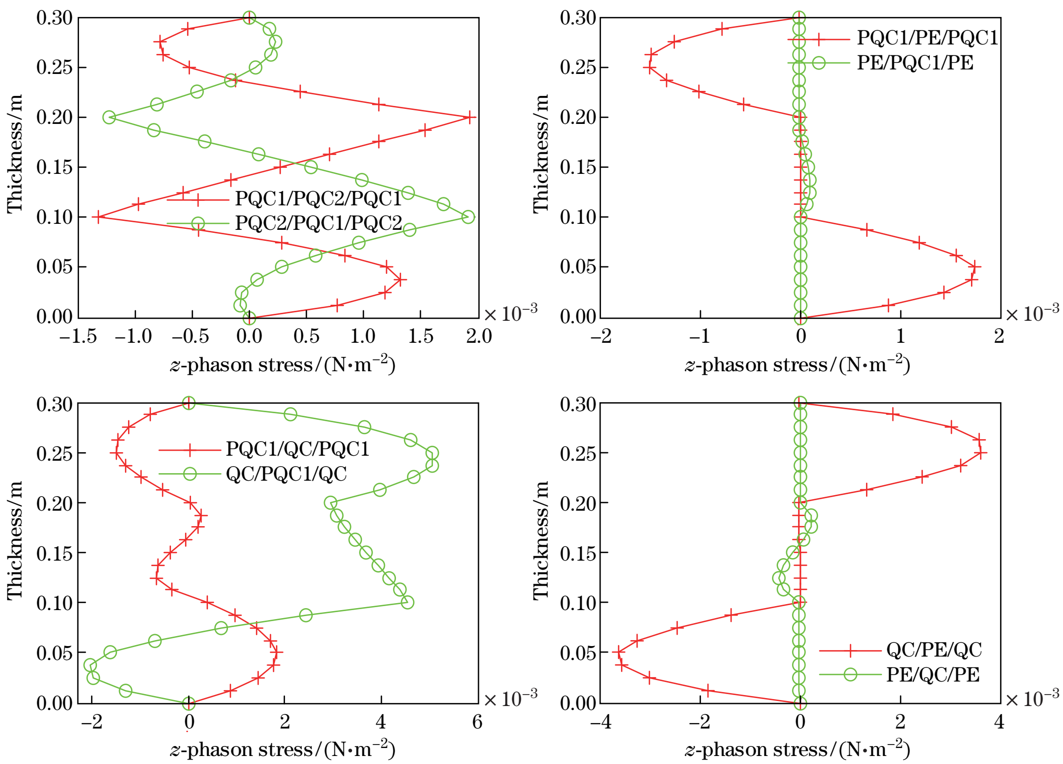

Fig. 8 Variation of phason normal stress H_{zz} along the thickness direction of the plate

sharply kinked across the interfaces. (ii) The stress of the phason field in the PE layer is always zero as expected. (iii) The stress of the phason field for PQC1/PQC2/PQC1 and PQC2/PQC1/PQC2 reaches its maximum at the interfaces, which is fully different from the other sandwich plates.

Figure 9 shows the variation of the electric displacement D_z for four different sandwich plates along the thickness direction of the plate under mechanical loads. It can be observed that the variation of the electric displacement is almost similar for four different plates. The electric displacement is always zero in the QC layer as expected.

Example 2 The plate subject to electrical loads on the top surface

Figures 10–12 show the variation of displacements of phonon and phason fields for four different sandwich plates along the thickness direction of the plates under electrical loads, respectively. It can be observed from Figs. 10 and 11 that the stacking sequence of the plates has a great effect on the displacements of phonon field under electrical loads and the displacements are kinked at the interfaces, which are different from those for mechanical loads (see Figs. 2 and 3). The variation of displacement of phason field under electrical loads (see Fig. 12) is similar to that for mechanical loads (see Fig. 4).

Figure 13 shows the variation of electric potential for four different sandwich plates along the thickness direction of the plates under electrical loads. It can be found that the stacking sequence has a great effect on the electric potential in the upper layers under electrical loads, which is also different from that for mechanical loads shown in Fig. 5.

Figures 14 and 15 illustrate the variation of shear and normal stresses of phonon field for four different sandwich plates along the thickness direction of the plates under electrical loads, respectively. It is interesting to note that the variations of the stresses of phonon field under electrical loads show the opposite trends when the stacking sequence is changed.

Figure 16 shows the variation of stress of phason field for four different sandwich plates along

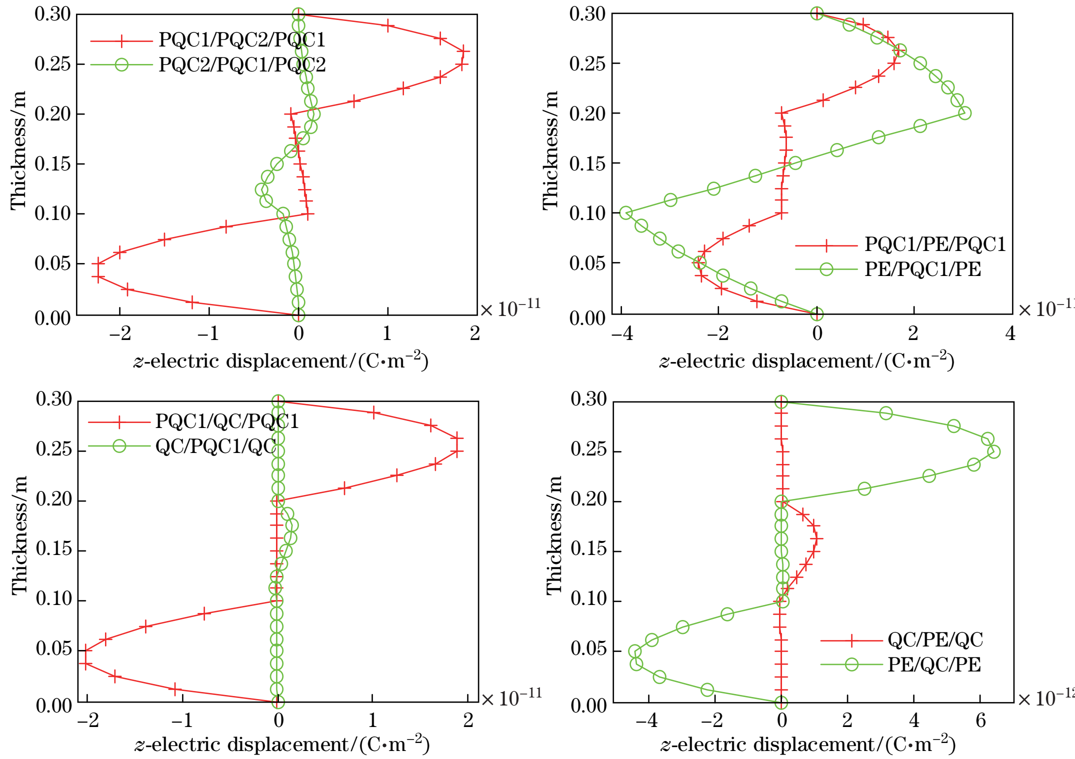

Fig. 9 Variation of electric displacement D_z along the thickness direction of the plate

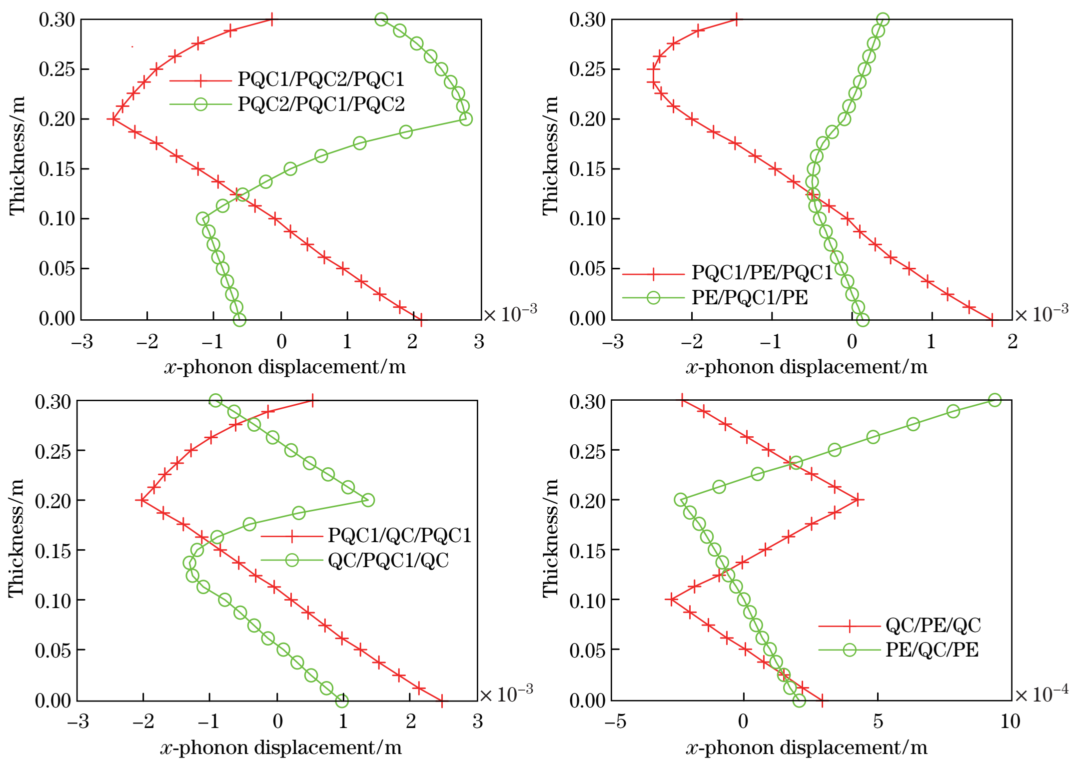

Fig. 10 Variation of phonon displacement $u_x (= u_y)$ along the thickness direction of the plate

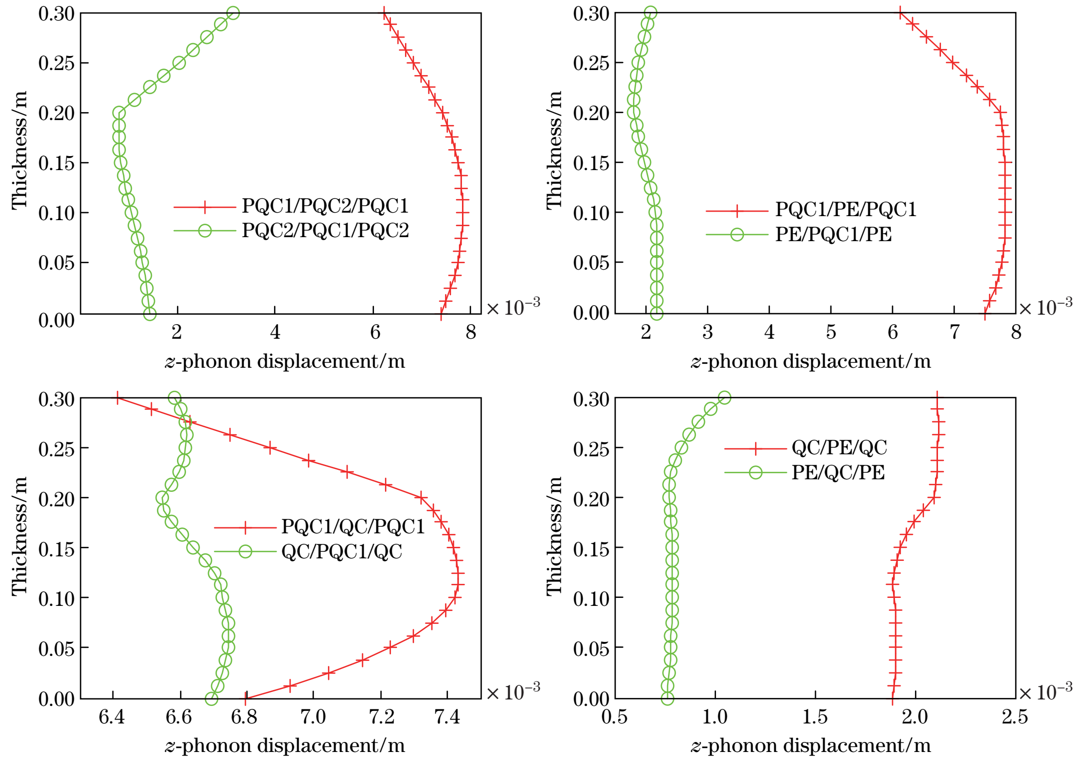

Fig. 11 Variation of phonon displacement u_z along the thickness direction of the plate

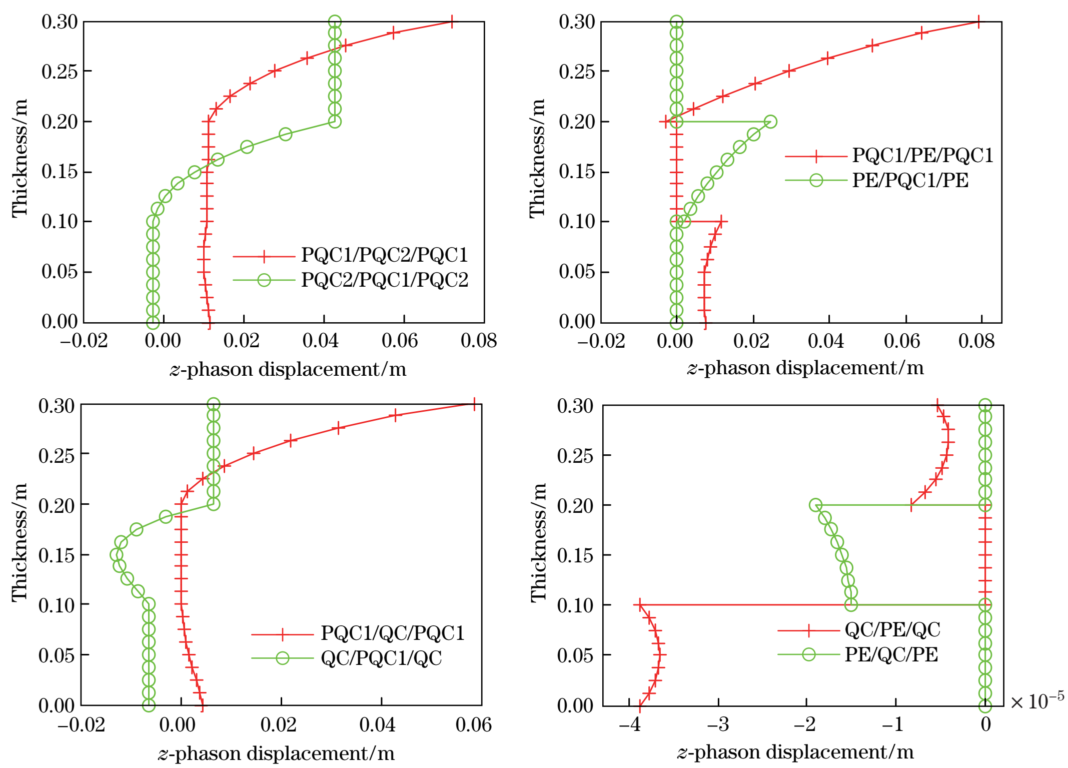

Fig. 12 Variation of phason displacement w_z along the thickness direction of the plate

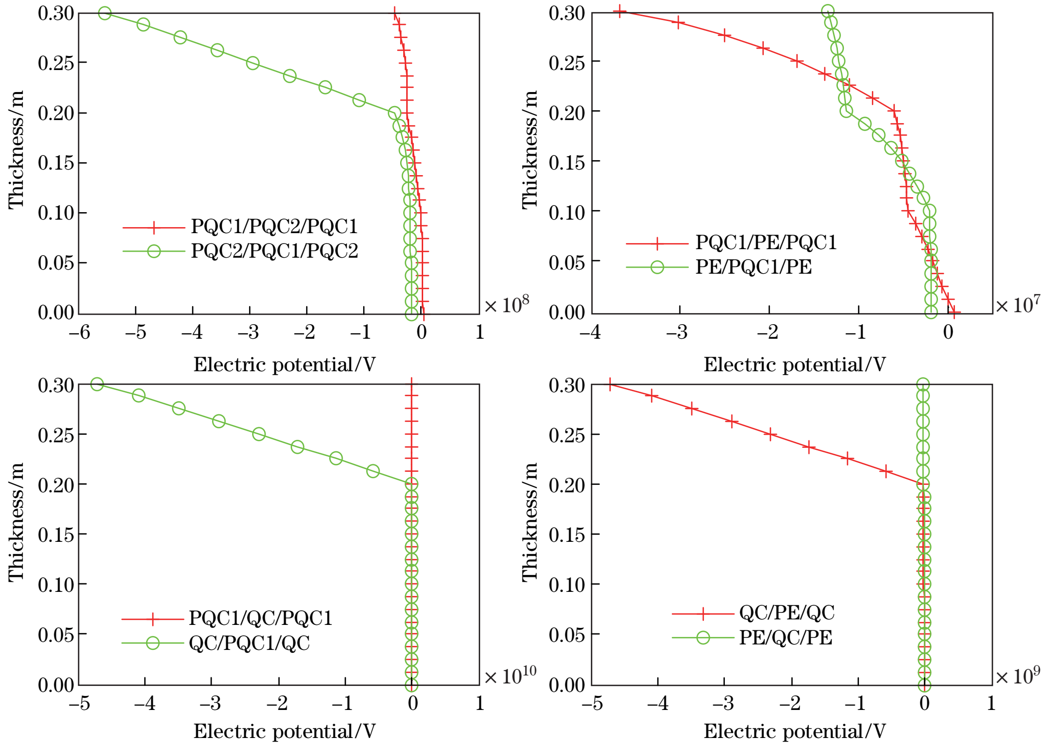

Fig. 13 Variation of electric potential ϕ along the thickness direction of the plate

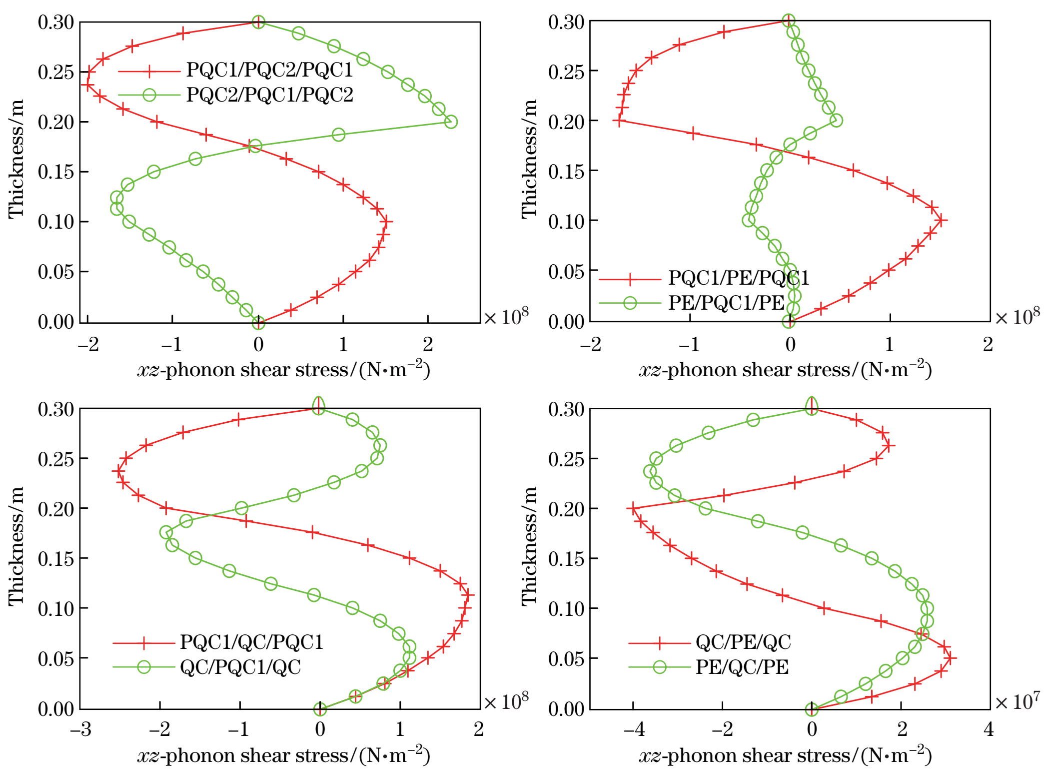

Fig. 14 Variation of phonon shear stress σ_{xz} along the thickness direction of the plate

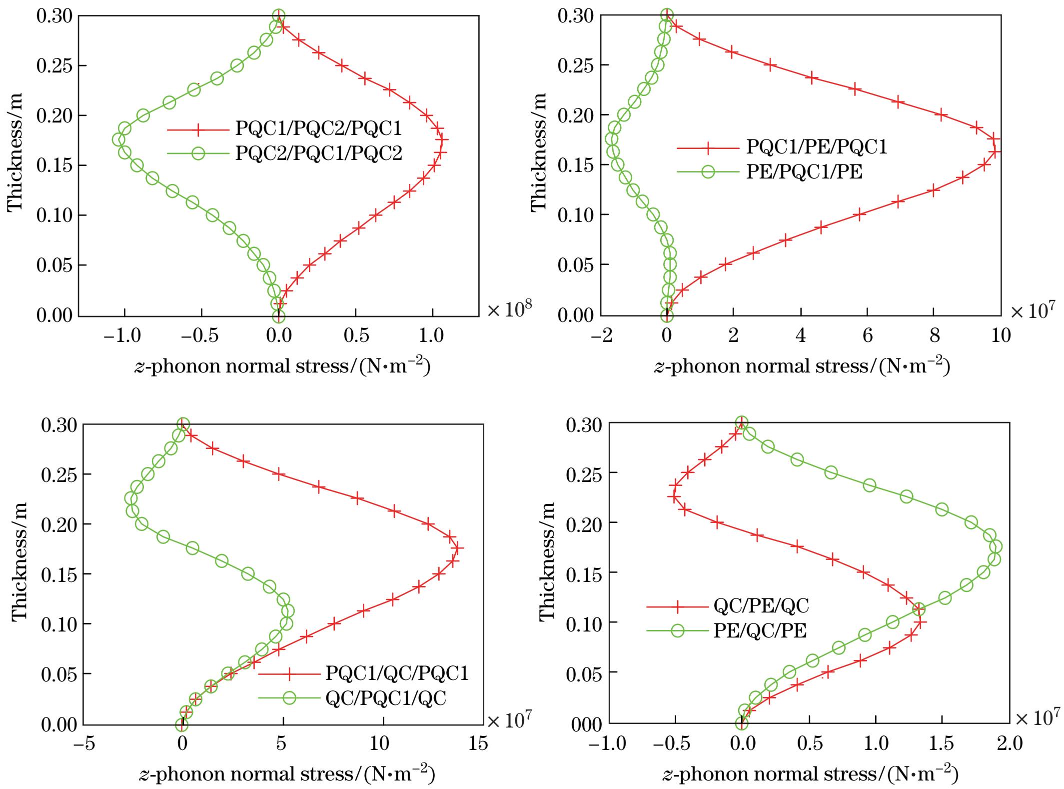

Fig. 15 Variation of phonon normal stress σ_{zz} along the thickness direction of the plate

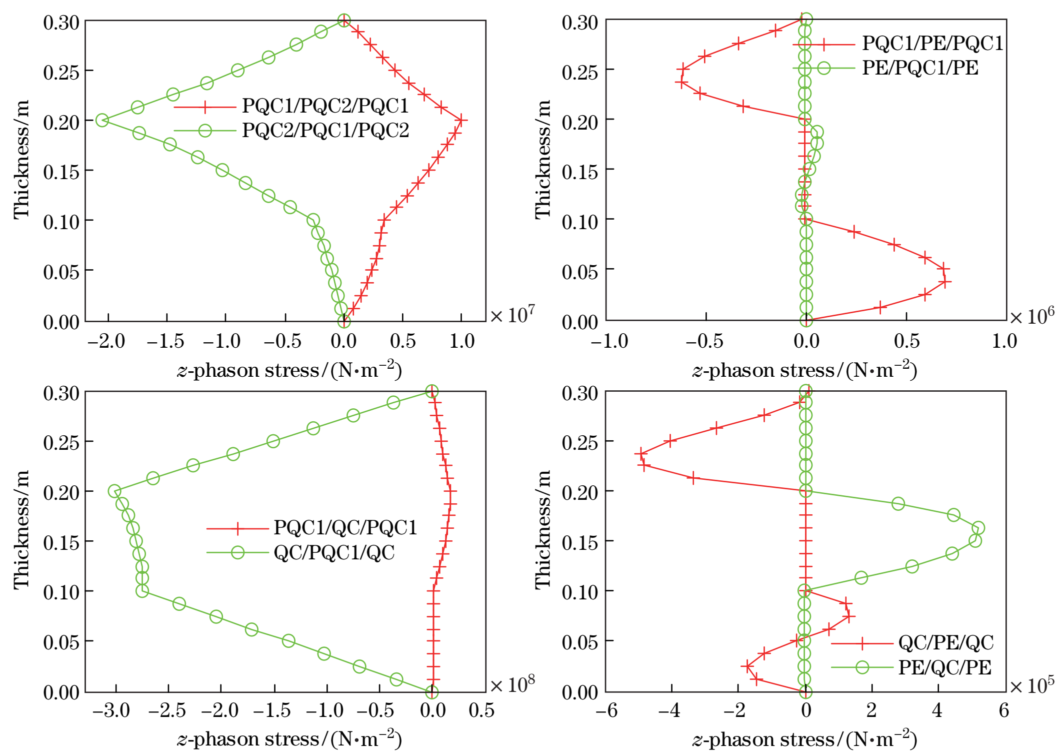

Fig. 16 Variation of phason normal stress H_{zz} along the thickness direction of the plate

the thickness direction of the plates under electrical loads. The stress of phason field in the PE layer is always zero, while it strongly depends on the stacking sequence in the other layers.

Figure 17 shows the variation of electric displacement for four different sandwich plates along the thickness direction of the plates under electrical loads. It can be seen that the stacking sequence has a large effect on the electric displacement in the upper two layers, while it has little influence on the electric displacement in the lower layer. The variation of electric displacement in all sandwich plates is similar except for PQC1/PE/PQC1 and PE/PQC1/PE plates.

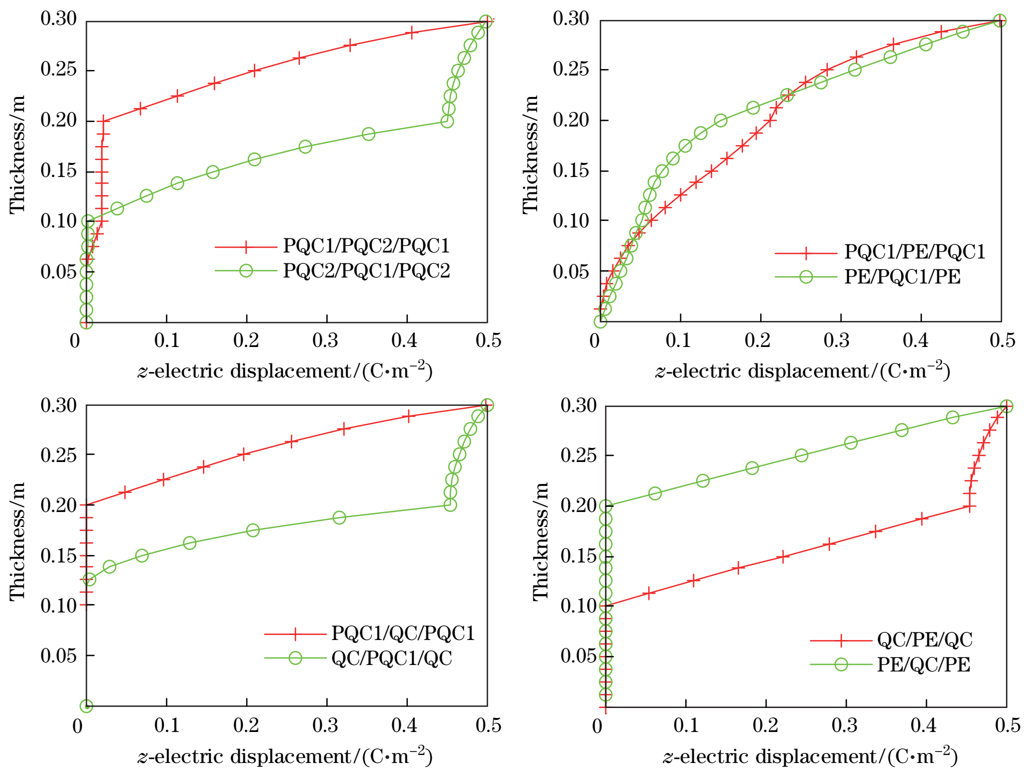

Fig. 17 Variation of electric displacement D_z along the thickness direction of the plate

As a special case, the present results can be reduced to the purely QC case[15] when the PE coefficients are zero and they can be reduced to the purely PE case[32] when the elastic constants of phason field are zero. Furthermore, the variations of u_z, σ_{zz}, σ_{xz}, D_z, and ϕ of sandwiches QC/PE/QC and PE/QC/PE under normal mechanical loads in this work are consistent with those in Fig. 13 by Yang et al.[32], which justifies correction of the present method.

6 Conclusions

By using the pseudo-Stroh formulism and propagator matrix method, a static deformation of a multilayered 1D hexagonal PQC plate is studied and the exact closed-form solutions of the extended displacement and traction for multilayered PQC plates are derived under surface mechanical and electrical loads. Numerical examples for four sandwich plates made of PQC, PE, and QC are provided to show the effect of stacking sequence on the phonon, phason, and electric fields. Some useful conclusions can be drawn.

(i) The stacking sequence of plates greatly affects the static deformation of the sandwich composite plates.

(ii) QCs are suitable for coatings or reinforcements in composites to enhance the mechanical property of the other composite materials as compared with PE materials.

(iii) The deformable responses of the layered plates under mechanical loads are fully different from those under electrical loads.

(iv) The electric potential for the sandwich plates QC/PE/QC and PE/QC/PE reaches its maximum at the interfaces under mechanical loads, while the electric potential of the other sandwich plates reaches its maximum on the surfaces.

References

[1] Shechtman, D., Blech, I., Gratias, D., and Cahn, J. W. Metallic phase with long-range orientational order and no translational symmetry. *Physical Review Letters*, **53**(20), 1951–1953 (1984)

[2] Pope, A., Tritt, T. M., Chernikov, M., and Feuerbacher, M. Thermal and electrical transport properties of the single-phase quasicrystalline material: $Al_{70.8}Pd_{20.9}Mn_{8.3}$. *Applied Physics Letters*, **75**(13), 1854–1856 (1999)

[3] Honda, Y., Edagawa, K., Yoshioka, A., Hashimoto, T., and Takeuchi, S. Al-Pd-Re icosahedral quasicrystals and their low electrical conductivities. *Japanese Journal of Applied Physics*, **33**(9A), 4929–4935 (1994)

[4] Zhou, C., Cai, F., Kong, J., Gong, S., and Xu, H. A study on the tribological properties of low-pressure plasma-sprayed Al-Cu-Fe-Cr quasicrystalline coating on titanium alloy. *Surface and Coatings Technology*, **187**(2/3), 225–229 (2004)

[5] Li, R., Li, Z., Dong, Z., and Khor, K. A. A review of transmission electron microscopy of quasicrystals — how are atoms arranged? *Crystals*, **6**(9), 105 (2016)

[6] Fleury, E., Lee, S. M., Kim, W. T., and Kim, D. H. Effects of air plasma spraying parameters on the Al-Cu-Fe quasicrystalline coating layer. *Journal of Non-Crystalline Solids*, **278**(1), 194–204 (2000)

[7] Dubois, J. M. Properties and applications of quasicrystals and complex metallic alloys. *Chemical Society Reviews*, **41**(20), 6760–6777 (2012)

[8] Tian, Y., Huang, H., Yuan, G., and Ding, W. Microstructure evolution and mechanical properties of quasicrystal-reinforced Mg-Zn-Gd alloy processed by cyclic extrusion and compression. *Journal of Alloys and Compounds*, **626**, 42–48 (2015)

[9] Li, R. T., Dong, Z. L., and Khor, K. A. Al-Cr-Fe quasicrystals as novel reinforcements in Ti based composites consolidated using high pressure spark plasma sintering. *Materials and Design*, **102**, 255–263 (2016)

[10] Gao, Y., Xu, S. P., and Zhao, B. S. Boundary conditions for plate bending in one-dimensional hexagonal quasicrystals. *Journal of Elasticity*, **86**(3), 221–233 (2007)

[11] Gao, Y. and Ricoeur, A. The refined theory of one-dimensional quasi-crystals in thick plate structures. *Journal of Applied Mechanics*, **78**(3), 2388–2399 (2011)

[12] Sladek, J., Sladek, V., and Pan, E. Bending analyses of 1D orthorhombic quasicrystal plates. *International Journal of Solids and Structures*, **50**(24), 3975–3983 (2013)

[13] Waksmanski, N., Pan, E., Yang, L. Z., and Gao, Y. Free vibration of a multilayered one-dimensional quasi-crystal plate. *Journal of Vibration and Acoustics*, **136**(2), 041019 (2014)

[14] Yang, L. Z., Gao, Y., Pan, E., and Waksmanski, N. An exact solution for a multilayered two-dimensional decagonal quasicrystal plate. *International Journal of Solids and Structures*, **51**(9), 1737–1749 (2014)

[15] Yang, L. Z., Gao, Y., Pan, E., and Waksmanski, N. An exact closed-form solution for a multilayered one-dimensional orthorhombic quasicrystal plate. *Acta Mechanica*, **226**(11), 3611–3621 (2015)

[16] Hu, C. Z., Wang, R., Ding, D. H., and Yang, W. Piezoelectric effects in quasicrystals. *Physical Review B*, **56**(5), 2463–2468 (1997)

[17] Fujiwara, T., Trambly, D. L. G., and Yamamoto, S. Electronic structure and electron transport in quasicrystals. *Materials Science Forum*, **150-151**, 387–394 (1994)

[18] Yang, W., Wang, R., Ding, D., and Hu, C. Elastic strains induced by electric fields in quasicrystals. *Journal of Physics Condensed Matter*, **7**(39), 499–502 (1995)

[19] Li, C. L. and Liu, Y. Y. The physical property tensors of one-dimensional quasicrystals. *Chinese Physics*, **13**(6), 924–931 (2004)

[20] Rao, K. R. M., Rao, P. H., and Chaitanya, B. S. K. Piezoelectricity in quasicrystals: a group-theoretical study. *Pramana*, **68**(3), 481–487 (2007)

[21] Altay, G. and Dökmeci, M. C. On the fundamental equations of piezoelasticity of quasicrystal media. *International Journal of Solids and Structures*, **49**(23/24), 3255–3262 (2012)

[22] Li, X. Y., Li, P. D., Wu, T. H., Shi, M. X., and Zhu, Z. W. Three-dimensional fundamental solutions for one-dimensional hexagonal quasicrystal with piezoelectric effect. *Physics Letters A*, **378**(10), 826–834 (2014)

[23] Yu, J., Guo, J., Pan, E., and Xing, Y. General solutions of plane problem in one-dimensional quasicrystal piezoelectric materials and its application on fracture mechanics. *Applied Mathematics and Mechanics* (*English Edition*), **36**(6), 793–814 (2015) https://doi.org/10.1007/s10483-015-1949-6

[24] Wang, X. and Pan, E. Analytical solutions for some defect problems in 1D hexagonal and 2D octagonal quasicrystals. *Pramana*, **70**(5), 911–933 (2008)

[25] Yang, L. Z., Gao, Y., Pan, E., and Waksmanski, N. Electriceelastic field induced by a straight dislocation in one-dimensional quasicrystals. *Acta Physica Polonica*, **126**(2), 467–470 (2014)

[26] Fan, C. Y., Li, Y., Xu, G. T., and Zhao, M. H. Fundamental solutions and analysis of three-dimensional cracks in one-dimensional hexagonal piezoelectric quasicrystals. *Mechanics Research Communications*, **74**, 39–44 (2016)

[27] Yu, J., Guo, J., and Xing, Y. Complex variable method for an anti-plane elliptical cavity of one-dimensional hexagonal piezoelectric quasicrystals. *Chinese Journal of Aeronautics*, **28**(4), 1287–1295 (2015)

[28] Yang, J. and Li, X. Analytical solutions of problem about a circular hole with a straight crack in one-dimensional hexagonal quasicrystals with piezoelectric effects. *Theoretical and Applied Fracture Mechanics*, **82**, 17–24 (2016)

[29] Guo, J., Zhang, Z., and Xing, Y. Antiplane analysis for an elliptical inclusion in 1D hexagonal piezoelectric quasicrystal composites. *Philosophical Magazine*, **96**(4), 349–369 (2016)

[30] Guo, J. and Pan, E. Three-phase cylinder model of one-dimensional hexagonal piezoelectric quasi-crystal composites. *Journal of Applied Mechanics*, **83**(8), 081007 (2016)

[31] Tupholme, G. E. One-dimensional piezoelectric quasicrystals with an embedded moving, non-uniformly loaded shear crack. *Acta Mechanica*, **228**(2), 547–560 (2017)

[32] Yang, L. Z., Li, Y., Gao, Y., Pan, E., and Waksmanski, N. Three-dimensional exact electric-elastic analysis of a multilayered two dimensional decagonal quasicrystal plate subjected to patch loading. *Composite Structures*, **171**, 198–216 (2017)

[33] Pan, E. Exact solution for simply supported and multilayered magneto-electro-elastic plates. *Journal of Applied Mechanics*, **68**(4), 608–618 (2001)

[34] Fan, T. Y. Mathematical theory and methods of mechanics of quasicrystalline materials. *Engineering*, **5**, 407–448 (2013)

[35] Lee, J. S. and Jiang, L. Z. Exact electroelastic analysis of piezoelectric laminae via state space approach. *International Journal of Solids and Structures*, **33**(7), 977–990 (1996)